Printed in the Republic of Korea
ANALYTICAL SCIENCE & TECHNOLOGY
Vol. 32 No. 4, 131-138, 2019
https://doi.org/10.5806/AST.2019.32.4.131

Investigation of physical characteristics for Al_2O_3:C dosimeter using LM-OSL

Myung-Jin Kim[1], Young-Ju Lee[2], Ki-Bum Kim[3], and Duk-Geun Hong[4,★]

[1]*Archaeological Science Institute, RADPION Inc., Daejeon 34013, Korea*
[2]*Radiation Technology Institute, Neosiskorea Co. Ltd., Daejeon 34122, Korea*
[3]*Institute of Liberal Education, Kangwon National University, Chuncheon 24341, Korea*
[4]*Dept. of Physics, Kangwon National University, Chuncheon 24341, Korea*
(Received May 11, 2019; Revised June 9, 2019; Accepted June 28, 2019)

Abstract This paper reports results on the physical properties of a powder type of Al_2O_3:C commonly used as a luminescence dosimeter using the LM-OSL technique. On the analysis with the general order kinetics model, the LM-OSL signal measured appeared to be composed of three components (fast, medium, slow) showing the largest area in the medium component. The photoionization cross sections of three components were distributed between 10^{-19}~10^{-21} cm^2. The values of the thermal assistance energy were evaluated the largest in slow component and the smallest in fast component, which indicates the electrons trapped in defects attributed to slow component should be the most sensitive to thermal vibration among three components. In illumination to blue light, the fast component showed a rapid linear decay and completely disappeared after light exposure time of about 5 s. The medium component decayed with two exponential elements but the slow component did not observed any noticeable change until light exposure time of 40 s. In a dose response study, all components exhibited a linear behaviour up to approximately 10 Gy.

Key words: Al_2O_3:C, LM-OSL, photoionization cross-section, thermal assistance energy, optical sensitivity, radiation response

1. Introduction

Al_2O_8:C is a compound, whose F center and F^+ center relate to luminescence emission exhibiting a very high intensity peak (dosimetric trap) near 200 °C on typical thermoluminescence (TL) glow curve, which was introduced in the 1990s for the purpose of developing a radiation dosimeter using TL[1]. The compound is highly sensitive to radiation to such an extent that it can degrade ~1 μGy of radiation, and thus, the compound has attracted attention for its potential in measuring environmental radiation, which requires low dosimetry. However, the compound has limitations in its thermal quenching effect, which shows a correlation between abnormal levels of radiation and luminescence intensity at high temperatures.[2] Recently, a method for radiation dosimetry using optically stimulated luminescence (OSL) that can overcome the thermal

★ Corresponding author
Phone : +82-(0)33-250-8473 Fax : +82-(0)33-259-5666
E-mail : dghong@kangwon.ac.kr

quenching phenomenon of Al_2O_8:C has been proposed and various research findings related to the compound have been reported.[3,4]

OSL that observes the luminescence emitted from the sample stimulated with light is classified according to the method of stimulation as follows. Continuous-wave OSL (CW-OSL) measures luminescence by continuously stimulating the sample with a constant output of light, linear modulation OSL (LM-OSL) measures luminescence while linearly increasing the output of the light, and pulsed OSL (POSL) measures luminescence after applying a short pulse of optical stimulus to the sample. The intensity of CW-OSL mainly used for radiation dosimetry is proportional to the radiation dose and decreases with measurement time. However, the luminescence signal measured using LM-OSL shows peak formation depending on the magnitude of the optical stimulation, where these peaks are related to the photoionization cross-section of the lattice defect (trap) present in the sample.[5,6] Additionally, POSL is commonly used to calculate the lifetime, indicating the duration time required for free electrons emitted from lattice defects due to optical stimulation combining with the recombination center and releasing the luminescence.[7]

In this study, the LM-OSL signal of Al_2O_3:C sample was measured, and then the photoionization cross-section of each component was calculated by decomposing the signal, which in turn was used to calculate thermal assistance energy that affects the energy distribution function of the lattice defects associated with each component. In addition, the photosensitivity and the response to radiation of each component were investigated for radiation-dosimetry using the LM-OSL signal.

2. Theory

In general, LM-OSL can be explained by energy band theory. Assuming a first-order kinetic model with no probability of lattice defects re-trapping electrons emitted by external stimuli in a sample composed of a single lattice defect and a single recombination center;[8] given that the output of the stimulus light source increased at a constant rate with time, the de-trapping rate of the electrons trapped in the lattice defect is expressed by the following equation.

$$\frac{dn(t)}{dt} = -\sigma\gamma t n(t) \tag{1}$$

In this equation, $\gamma = I_0/T$ is the rate at which the output of the stimulus light source constantly increases with time and T is the total luminescence measurement time. As the flux of the stimulus light source is represented by $\Phi(t) = \gamma t$, the signal of LM-OSL appears as follows.

$$L(t) = -\frac{dn(t)}{dt} = n_0\gamma t \exp\left(-\frac{1}{2}\sigma\gamma t^2\right) \tag{2}$$

Here, n_0 is the initial number of electrons trapped in the lattice defect and σ is the photoionization cross-section of the lattice defect. Also, the maximum peak point (L_{max}) of the LM-OSL signal and the time (t_{max}) at the maximum peak point can be obtained using Eq. (2) as follows.

$$t_{max} = \sqrt{\frac{1}{\sigma\gamma}} \tag{3}$$

$$L_{max} = n_0\sqrt{\sigma\gamma}\exp\left(-\frac{1}{2}\right) = 0.607\frac{n_0}{t_{max}} \tag{4}$$

However, in contrast to the previous assumption, assuming a general order kinetic model that considers the probability that electrons emitted from the lattice defects are re-trapped in the lattice defects, the electron emission rate with increasing output of stimulus light source is given by Eq. (5).[9]

$$\frac{dn(t)}{dt} = -\alpha\gamma t n^{\beta}(t) \tag{5}$$

Here, $\alpha = \sigma/n_0^{\beta-1}$ and β is a dimensionless coefficient that is neither 0 nor 1. The signal of the LM-OSL in this case is shown below.

$$L(t) = -\frac{dn(t)}{dt} = n_0\sigma\gamma t\left[(\beta-1)\frac{1}{2}\sigma\gamma t^2 + 1\right]^{\beta/(1-\beta)} \tag{6}$$

Furthermore, the maximum peak point (L_{max}) of LM-OSL and the time at the peak point (t_{max}) are as follows.

$$t_{max} = \sqrt{\frac{2}{\sigma\gamma(\beta+1)}} \tag{7}$$

$$L_{\max} = \frac{2n_0}{\beta+1}\frac{1}{t_{\max}}\left(\frac{2\beta}{\beta+1}\right)^{\beta/(1-\beta)} \quad (8)$$

The LM-OSL signal can be de-convoluted into a linear combination of the first or general order kinetic model, since the maximum points of the peaks can be separated according to the stimulation time, and thus, provide information on the number of electrons trapped in the lattice defects of each decomposed component and the size of the photoionization cross-section.[10]

3. Samples and Experimental Equipment

This study used Al_2O_3:C powder (< 105 μm) manufactured by Landauer, USA as samples. The LM-OSL signal was measured with an automated Risø TL/OSL reader (Risø TL/OSL-DA-20) from the Risø laboratory in Denmark installed in the Central Laboratory of Kangwon National University.[11] A blue light emitting diode (Nichia type NSPB-500S, 470 ± 20 nm) was used as the stimulus light source and the maximum power output of the light source was 50 mW/cm^2. The LM-OSL signal was detected by the photomultiplier tube (EMI 9635QA) attached a Hoya U-340 filter. The sample was irradiated from ^{90}Sr/^{90}Y beta source, and the radiation dose rate was approximately 0.08 Gy/s.

4. Results and Discussion

4.1. LM-OSL measurement and photoionization cross-section

While the CW-OSL signal that stimulates the sample with constant output from a stimulus light source exponentially decreases over time, the LM-OSL signal that stimulates the sample with linearly increasing output leads to peaks according to time. The LM-OSL signal in peak form can be represented by a mathematical linear combination of the selected kinetic model. It can be represented as Eq. (9) when the first order kinetic model has been selected, and Eq. (10) when the general order kinetic model has been selected.

$$L(t) = \sum_{i=1}^{N} L_i = \sum_{i=1}^{N} n_{0i}\sigma_i\gamma t\ \exp\left(-\frac{1}{2}\sigma_i\gamma t^2\right) \quad (9)$$

$$L(t) = \sum_{i=1}^{N} L_i = \sum_{i=1}^{N} n_{0i}\sigma_i\gamma t\left[(\beta-1)\frac{1}{2}\sigma_i\gamma t^2+1\right]^{\beta/(1-\beta)} \quad (10)$$

It is very important to determine the kinetic order to separate the exact components of the LM-OSL signal. In examining the previous studies on the kinetic order of Al_2O_3:C, Whitley and McKeever[12] decomposed the LM-OSL signal into three components with the first-order kinetic model, while Dallas *et al.*[9] approached the component decomposition of the LM-OSL signal using the general order kinetic model of three components. The kinetic order determination process performed in this study was intended to mathematically decompose the LM-OSL signal by an optimal combination of variables through repeatedly substituting appropriate parameters into Eqs, (9) and (10). The suitability of the signal decomposition by the final combination of variables was determined by considering the figure of merit ($FOM(\%) = \frac{\sum|I_{\exp}-I_{dec}|}{\sum I_{\exp}}\times 100$). The sequence was performed using the non-linear least squares method applying the Levenberg-Marquardt algorithm employing the Origin (version 6.1) program.

In this study, the beta dose of 0.1 Gy was irradiated to the sample as the first step to calculate the photoionization cross-section of Al_2O_3:C sample from the LM-OSL signal. The LM-OSL signal was measured by linearly increasing the intensity of the stimulus light source from 0 to 90 % for 3600 seconds while keeping the sample constant at 120 °C, in order to remove the interference caused by unstable lattice defect (see *Fig.* 1). The results of the decomposition of the measured LM-OSL signal showed that the LM-OSL signal was decomposed into three components and in this case, the FOM values of the first-order kinetic model and the general order dynamic model were 11.2 % and 1.5 %, respectively. This implies that in the case of Al_2O_3:C samples used in this study, the approach using the general order kinetic

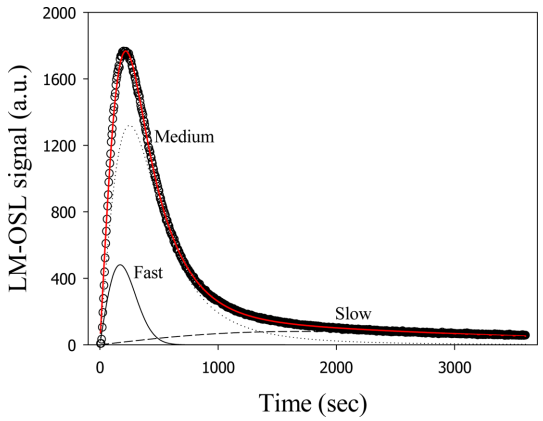

Fig. 1. An example of LM-OSL signal measured from Al_2O_3:C dosimeter and peak deconvolution using the general order kinetics.

model may be more reliable than the first-order kinetic model.

Fig. 1 shows an example of decomposing the measured LM-OSL signal using the general-order kinetic model of Eq. (10). The decomposed components were named as fast (F), medium (M) and slow (S) components, respectively, depending on the magnitude of the photoionization cross-section, and the data imply that the intensity of the medium component is the highest. The photoionization cross-section of each component of the Al_2O_3:C sample calculated from the LM-OSL signal decomposition was 10^{-19} ~ 10^{-21} cm^2, and the results are summarized in *Table* 1.

4.2. Thermal assistance energy

The electron-phonon coupling phenomenon in inorganic crystals widens the energy distribution function of lattice defects and changes photoionization characteristics by photons. In other words, electrons can be released from lattice defects by somewhat lower photon energy due to the increase in phonon energy from the heat. This thermal dependence is called thermal assistance,[13] and in the case of LM-OSL it can be calculated from the thermal dependence of the photoionization cross-section.[14,15]

$$\sigma = \sigma_\infty \exp\left(-\frac{E^*}{k_B T}\right), E^* = \phi(E_0 - h\nu) \quad (11)$$

In the equation above, σ_∞ is the magnitude of the photoionization cross-section when is $T = \infty$, E_0 is the energy gap, $h\nu$ is the photon energy of light source

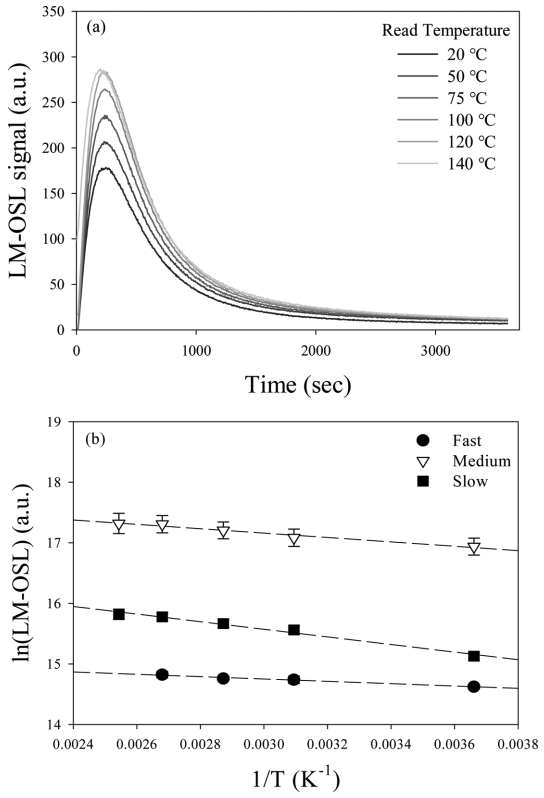

Fig. 2. (a) LM-OSL signal according to measuring temperature (b) ln(LM-OSL) versus 1/T to obtain value of thermal assistance energy.

Table 1. Physical characteristics evaluated from the LM-OSL measurements of Al_2O_3:C dosimeter

Component	Trapped number n_0	Photoionization cross-section σ (120 °C, cm^2)	Kinetics order β	Thermal assistance energy E^* (eV)	Photoionization cross-section by Whitley and Mckeever[12]
Fast	1.17×10^7	7.2×10^{-19}	2	0.017	$5.8 \sim 7.0 \times 10^{-19}$
Medium	1.11×10^8	1.5×10^{-19}	1.0045	0.031	$1.4 \sim 1.7 \times 10^{-19}$
Slow	3.73×10^7	2.9×10^{-21}	2	0.054	$3.3 \sim 3.7 \times 10^{-20}$

for optical pumping, and k_B is the Boltzmann constant.

In this study, Al_2O_3:C samples were irradiated with 0.1 Gy beta radiation to observe the thermal assistance of Al_2O_3:C samples and each LM-OSL signal was measured for 3600 seconds while sequentially increasing the measurement temperature to 20, 50, 75, 100, 120, and 140 °C. As shown in *Fig.* 2(a), the LM-OSL intensity of Al_2O_3:C samples also increased as the measurement temperature increased. This suggests that there exists a thermal assistance phenomenon in the Al_2O_3: C sample.

In general, when the LM-OSL signal can be represented as a linear combination of the first-order kinetic model as shown in Eq. (9), the LM-OSL signal intensity and the photoionization cross-section are directly correlated. Therefore, the thermal assistance energy E^* can be easily calculated from the change in the LM-OSL signal intensity according to the measured temperature. However, the LM-OSL signal of the Al_2O_3:C sample measured in this study is decomposed into the general order kinetic component of Eq. (10), which makes it difficult to calculate the direct thermal assistance energy. Therefore, the thermal assistance energy value calculated using the general order kinetic model in this study was used as the data to compare the relative sizes of electron-phonon bonds among the components.

To observe in detail the thermal assistance of Al_2O_3:C samples based on these assumptions, the LM-OSL signal obtained at each measurement temperature was decomposed by three (fast, medium, slow) general-order kinetic components. The results showed that the intensity of each component increased with the measured temperature. If this was expressed as a function of ln(LM-OSL) and 1/T as shown in *Fig*. 2(b), the intensity of each LM-OSL component appears linear with the measured temperature. Therefore, the thermal assistance energy E^* of each component was directly calculated using Eq. (12).

$$\ln(L) = \ln(L_\infty) - \frac{E^*}{k_B} \cdot \frac{1}{T} \tag{12}$$

Table 1 summarizes the thermal assistance energy of each component of Al_2O_3:C calculated by linear regression analysis using the linear function of Eq. (12). As a result, the thermal assistance energy of the fast component was the smallest, followed by the medium component, and then, the slow component. This suggests that the electron-phonon bonds of fast and medium components, which are mainly used for the calculation of the radiation dose, are relatively weak, and thus, the electrons trapped in these lattice defects are less sensitive to the lattice vibration caused from heat. Therefore, to overcome the thermal quenching phenomenon of Al_2O_3:C materials and to improve the accuracy of the dosimetry, the use of OSL with heat stability is required.

4.3. Reduction of LM-OSL due to light exposure

To investigate the sensitivity of the LM-OSL signal

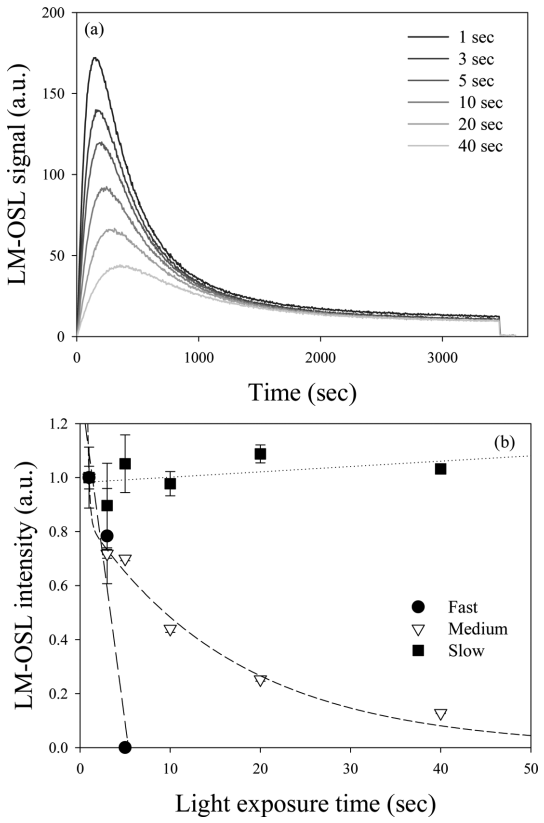

Fig. 3. (a) LM-OSL signal according to light exposure time (b) LM-OSL intensity against light exposure time for each LM-OSL component.

to light on the Al_2O_3:C sample, Al_2O_3:C samples irradiated with 0.1 Gy beta radiation were prepared. Before the measurement of LM-OSL, the samples were exposed to light using a blue light emitting diode by sequentially increasing irradiation time for 1, 3, 5, 10, 20, and 40 seconds, and measured for LM-OSL signals for 3600 seconds at a measurement temperature of 120 °C. As shown in *Fig.* 3(a), the LM-OSL signal intensity of the Al_2O_3:C sample rapidly decreased as light exposure time increased.

To analyze the photosensitivity of Al_2O_3:C samples in detail, the LM-OSL signals measured from the samples with different light exposure times were decomposed into three (fast, medium, slow) general order kinetic components. As a result, as shown in *Fig.* 3(b), the fast component with the largest photoionization cross-section disappeared as the LM-OSL signal decreased linearly within 5 seconds of light exposure, and the LM-OSL signal of the medium component declined exponentially. However, no significant change was observed in LM-OSL signal intensity of the slow component in up to 40 seconds of light exposure. This shows that the sensitivity of the Al_2O_3:C luminescent signal to light is directly related to the photoionization cross-section obtained as a result of this study. In the case of the exponentially decreasing medium component LM-OSL signal, curve fitting using linear combinations of two exponential functions was performed as shown in Eq. (13).

$$L_{medium} = \sum_{i=1}^{2} a_i \exp(b_i t) \quad (13)$$

The phenomenon of two exponential decays of the medium component is considered to be due to the phototransfer phenomenon (a phenomenon in which electrons in a lattice defect by light irradiation do not directly move to a recombination center after being transferred to a conduction band, but are re-trapped in a lattice defect and are then moved to a recombination center via a conduction band by continuous light irradiation to emit luminescence)[18] in the luminescence process.

4.4. Radiation response of LM-OSL signal

To observe the radiation reactivity of the LM-OSL signal to Al_2O_3:C samples, LM-OSL signals were measured for 3600 seconds at 120 °C in samples irradiated with 0.24, 0.48, 0.96, 4.8, and 9.6 Gy. As shown in *Fig.* 4(a), the LM-OSL signal intensity of the Al_2O_3:C sample also increased with an increase in the radiation dose. This means that the radiation response of the LM-OSL signal to the Al_2O_3:C sample is excellent.

To thoroughly investigate the radiation reactivity of Al_2O_3:C samples, the LM-OSL signal obtained from each dose was decomposed into three (fast, medium, slow) general order kinetic components, which was made as a function of radiation dose and LM-OSL signal intensity. As shown in *Fig.* 4(b), the dose response curve of the LM-OSL signal linearly

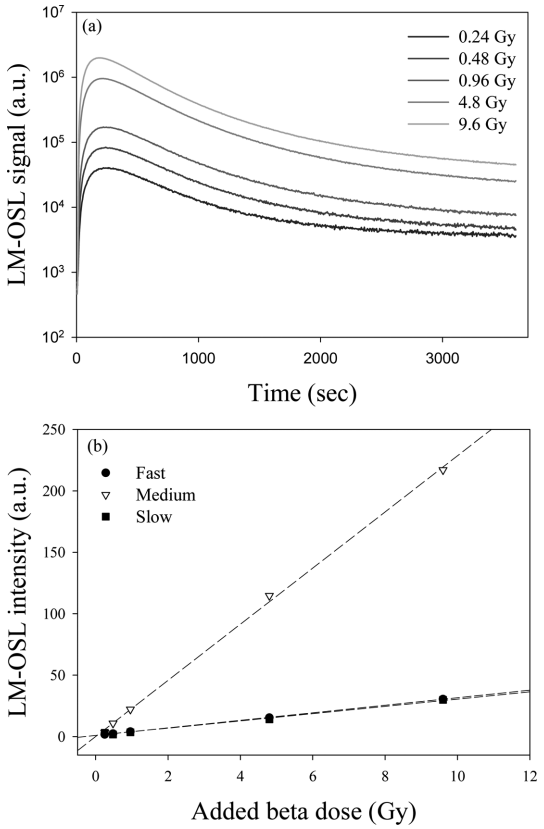

Fig. 4. (a) LM-OSL signal after the various radiation doses (b) Dose response curves of each LM-OSL component.

increased to more than 8 Gy of lethal dose ($LD_{100/60}$) for all components. In particular, the dose response was 2.29×10^7 counts/Gy in the case of the medium component occupying the largest area of the LM-OSL signal (see *Fig.* 1), which is more than 7 times higher than that of the fast component of 3.20×10^6 counts/Gy.

5. Conclusions

In this study, the LM-OSL signal of the Al_2O_3:C sample was measured, and the photoionization cross-section of each component was calculated by decomposing the signal, which in turn was used to calculate the thermal assistance energy of each component. The photosensitivity and the reactivity to radiation of the decomposed components were also investigated. As a result of LM-OSL measurement, the Al_2O_3:C sample was decomposed into three general-order kinetic components (fast, medium, slow). The medium area was the largest and the photoionization cross-section of each component was distributed in the range of $10^{-19} \sim 10^{-21}$ cm^2. The thermal assistance energy of these components was the lowest in the fast component, followed by the medium component, and then the slow component. This suggests that electrons trapped in these lattice defects are less sensitive to lattice vibrations due to heat, since the electron-phonon bonds of fast and medium components, mainly used for calculating radiation dose, are relatively weak. From the photosensitivity of the Al_2O_3:C sample, the fast component with the greatest photoionization cross-section area linearly decreased within approximately 5 seconds of light exposure time and disappeared. In addition, the LM-OSL signal of the medium component was reduced exponentially in the two components, and the LM-OSL signal intensity of the slow component was not significantly changed until the light exposure time reached 40 seconds. Finally, results of the investigation on the radiation reactivity of the LM-OSL signal showed that the dose response curve of the LM-OSL signal linearly increased for all the components up to approximately 10 Gy irradiation and the dose response of the medium component, which occupied the largest area of the LM-OSL signal, was excellent at 2.29×10^7 counts/Gy. The photoionization cross-section, thermal assistance energy, photosensitivity and radiation reactivity of each component of LM-OSL for the Al_2O_3:C sample evaluated in this study can be used as the fundamental information for calculation of radiation dose using OSL signal of Al_2O_3:C.

Acknowledgements

This research was supported by 2017 Research Grant from Kangwon National University (No. 520170484) and Basic Science Research Program through the National Research Foundation of Korea (NRF) funded by the Ministry of Education, Science and Technology (NRF-2017R1D1A1B03029608).

References

1. M. S. Akselrod, N. Agersnap Larsen, V. Whitley and S. W. S. Mckeever, *J. Appl. Phys.*, **84**(6), 3364-3373 (2012).
2. M. S. Akselrod, V. S. Kortov, D. J. Kravetsky and V. I. Gotlib, *Radiat. Prot. Dosim.*, **33**(1), 119-122 (1990).
3. S. W. S. Mckeever, *Nucl. Instr. Methods Phys. B*, **184**, 29-54 (2011).
4. J. M. Edmund and C. E. Andersen, *Radiat. Meas.*, **42**, 177-189 (2007).
5. E. Bulur, *Radiat. Meas.*, **26**(5), 701-709 (1996).
6. E. Bulur, L. Botter-Jensen ,and A. S. Murray, *Radiat. Meas.*, **33**, 715-719 (2001).
7. M. L. Chithambo, *J. Phys. D: Appl. Phys.*, **40**. 1874-1879 (2007).
8. R. Chen and S. W. S. Mckeever, 'Theory of thermoluminescence and related phenomena', World Scientific Publishing, 1997.
9. G. I. Dallas, G. S. Polymeris, E. C. Stefanaki, D. Afouxenidis, N. C. Tsirliganis, and G. Kitis, *Radiat. Meas.*, **43**, 335-340 (2008).
10. E. Bulur, L. Botter-Jensen, and A. S. Murray, *Radiat. Meas.*, **32**, 407-411 (2000).
11. L. Botter-Jenson, E. Bulur, G. A. T. Duller, and A. S.

Murray, *Radiat. Meas.*, **32**, 523-528 (2000).
12. V. H. Whitley and S. W. S. Mckeever, *Radiat. Prot. Dosim.*, **100**(1-4), 61-66 (2002).
13. N. A. Spooner, *Radiat. Meas.*, **23**, 593-600 (1994).
14. F. Urbach, *Phys. Rev.*, **92**, 1324 (1953).
15. M. J. Kim, K. W. Song, and D. G. Hong, *SAEMULLI*, **53**, 171-177 (2006).
16. M. L. Chithambo, C. Seneza, and J. M. Kalita, *Radiat. Meas.*, **105**, 7-16 (2017).

Authors' Positions

Myung-Jin Kim : CTO (Chief Technical Officer)
Young-Ju Lee : Researcher
Ki-Bum Kim : Professor
Duk-Geun Hong : Professor